Results in Physics 12 (2019) 46–51

Contents lists available at ScienceDirect

Results in Physics

journal homepage: www.elsevier.com/locate/rinp

Morphology evolution of self-organized porous structures in silicon surface

Joon-Gon Son[a], Jung Won Choi[b], Okkyun Seo[c], Do Young Noh[a,*], Do-Kyeong Ko[a,*]

[a] Department of Physics and Photon Science, Gwangju Institute of Science and Technology, Gwangju 61005, Republic of Korea
[b] School of Materials Science and Engineering, Gwangju Institute of Science and Technology, Gwangju 61005, Republic of Korea
[c] Synchrotron X-ray Station at SPring-8, Research Network and Facility Services Division, National Institute for Materials Science (NIMS), Kouto, Sayo, Hyogo 679-5148, Japan

ARTICLE INFO

Keywords:
Porous surface
Self-organization
LIPSS

ABSTRACT

We have investigated the morphology evolution of silicon surface by laser irradiation. A pulsed ns-laser interaction with silicon in aqueous medium can produce self-organized microporous concave cell array structure without any chemicals and auxiliary equipment. Low radiant power was applied to the photo-induced non-thermal silicon surface modification. At the early stage, hemispherical patterns of 2 ~ 3 μm were formed, maintaining a constant distance from each other without merging. Due to the thermal properties of water, subsurface heating proceeds under the silicon surface. The molten surface leads to the surface modulation to form subsided areas or expansions by nucleation and coalescence, resulting in the formation of a concave cone-shaped porous surface with a diameter of 10 ~ 20 μm. The AFM reveals that the hierarchical hemispherical structures of two different scales are progressing simultaneously from the early stage.

Introduction

Silicon is the abundant element on earth and has been widely used for various applications since industrial technology has developed over the past several decades. Many special functions are given by morphological changing process, especially for porous silicon. It is available for the state-of-the-art research such as anti-reflective optical absorber in solar cell [1], light emission element in display device [2], scaffold for tissue regeneration in biomechanics [3], chemical and bio-sensor [4], and so on. Making the porous structure on the surface of metal or semiconductor with chemical or optical methods are well known. For example, anodic electrochemical dissolution in HF solution, etches Si in mixtures of HF [5,6] and HNO_3. Lithography with photomask, and etching with the template are also currently in use [7]. However, these have disadvantages of employing complicated preparations and toxic chemicals.

Since laser technology has developed, many new phenomena for wide interactions with materials have been explored recently. For the peculiarity of delivering intensive energy by the form of photon within the short duration, laser easily makes material ablation and re-deposition through solidification. As a result of interaction between laser and matter, nanoparticle and laser-induced periodic surface structure (LIPSS) can be formed after interaction, which can be explained with capillary waves [8], optical interference (between the incident and scattered light or surface plasmons at the surface) [9] and so forth. Fundamentally, it is happening from the process of absorbed energy dissipation. Absorbed photon can penetrate the material with creating the phonon by lattice coupling. Radiated thermal energy produce the thermodynamic effect to weaken the molecular bonding and remains some traces in substance, such as Rayleigh-Benard convection [10], Marangoni convection [11] and etc., which are the type of naturally self-organized formation. The small amount of thermal energy can be dissipated from the particlization by expanding the surface or from the vaporization by mass removal with thermal energy. Large energy penetrates the certain depth of layers, which causes the volume heating to make the state of superheated liquid by increasing the temperature higher than surface temperature. Subsequently, the expansion by nucleation [12] and explosion [13] enables to eject the molten material inside then remains the crater.

In this letter, we have attained micro-scaled porous structure with laser exposure onto silicon wafer under aqueous media. We focused on the low radiant power regime and observed convective thermodynamic effect by photo-induced phonon-coupled thermal radiation purely without any plasma, recoil pressure and annealing. We investigated the morphology evolution of exposed surface with time variation and discussed physical mechanism related to the self-organized formation and structure.

* Corresponding authors.
E-mail addresses: dynoh@gist.ac.kr (D.Y. Noh), dkko@gist.ac.kr (D.-K. Ko).

https://doi.org/10.1016/j.rinp.2018.11.006
Received 30 October 2018; Accepted 2 November 2018
Available online 14 November 2018

Material and methods

Commercial p-type single crystalline (1 0 0) Si wafers (Virginia Semiconductor) with resistivity of 20–25 Ω·cm and thickness of 600 ± 25 μm were cleaved into small chips for target samples. A second harmonic Q-switched Nd-YAG laser (Quantel Co., Ultra) was equipped to generate 532-nm nanosecond (< 10 ns) pulses with a repetition rate of 20 Hz which has a Gaussian beam profile approximately. Dichroic mirror was employed to separate source beam into 532 nm wavelength. The silicon samples were set vertically on the side wall inside the square quartz cuvette (Hellma, 1 × 1 × 4 cm^3) filled with 1 mℓ of DI water. A Laser beam with the flux of 0.34 J/cm^2 passed through the side of the cuvette cell was irradiated normally onto the surface of the Si target. We analyzed surface morphology of silicon samples at different exposure time varied from 10 s to 1 h.

In order to check the effect of the cuvette cell, experiments were carried out to irradiate the laser beam through the water vertically onto the Si sample placed on the bottom of the reservoir. The results showed a negligible difference, and the experiments proceeded in the cuvette cell.

To observe the surface morphology changes of irradiated silicon, a scanning electron microscope (SEM, JEOL 7500F) was exploited. For a more detailed inspection of surface roughness, an atomic force microscope (AFM, NT-MDT Co., Solver) was also used.

Results & discussion

Overall, the surface morphology modulation by laser exposure in water medium manifest two distinct phases of different scale. At the early stage, donut-like structure with 3-μm diameter (conveniently, local expansion) that has an inner diameter of 1 μm appears sporadically with the ripple pattern (in Fig. 1a-1c). Fig. 1 shows the surface modification depends on the exposure time from 30 s to 3 min. Surface modulation can be found faintly even at 10 s after the exposure, whereas the relief of entire pattern is getting clear after 50 s and developed into inflated roughness after 2 min. Interestingly, local expanded unit cell does not seem to be enlarged with merging others, but it keeps the balance of size and distance between themselves closely. Hence, filling the whole area with uniform unit cells establishes the typical Turing Pattern [14,15] implies that the thermal energy exchange is effectively activated and the dominant mechanism of energy transfer on the surface is not by diffusion but by waves. In the image of 3-minute exposure (Fig. 1d), relatively large scaled expansions of 10–20 μm diameter (macro expansion) appears. It is a contrast to the local expansion with the period of 2 μm, which starts with the larger convective current inside and a thickened molten layer originated by local instability.

After 4-minute exposure, macro expansions are primarily produced while local expansions become indistinct (see Fig. 2a and b). The explosions from the surface are displayed with the radially extruded side around the entrance of a deep hole and nano-scaled debris which were found around the exploded structure. Such a submicron structure is vaporized and changed to smooth shape as time passes. Fig. 2c shows that both macro and local modulation exist together in this region, but the center of macro structure is subsided instead of making explosions. Fig. 2d, which is an enlarged picture of Fig. 2c, shows a concave structure which is the earliest stage of the hole formation. Fig. 2e shows the concave structure with a hole and the early stage of concave cell together. Basically, location of macro unit cell formation follows the distribution of Rayleigh-Benard convection that is rising on the edges and sinking into the center of the cell in this case [15]. Besides, this fluctuation occurs at the interface between two fluids of different densities [16]. When the lighter fluid pushes the heavier fluid, expansion-like bubble flows upward and sinking hole flows downward [17].

Once the surface is modulated, absorbed energy is relatively decreased at the inclined surface, whereas in the area on top and bottom it is increased. Consequently, the molten region of the concave bottom spreads along the periphery wall and sinks downward. Due to the effect of high density energy localization by surface reflective focusing, a deeper hole is created in the bottom area [18]. Macro-scaled unit cells are going to be crowded and become the concave structure of diameter 10–20 μm surrounded by separation walls afterward. Finally, they transform into distorted hexagonal cells in irregular arrangement (as shown in Fig. 2f). It is a similar manner with the well-known

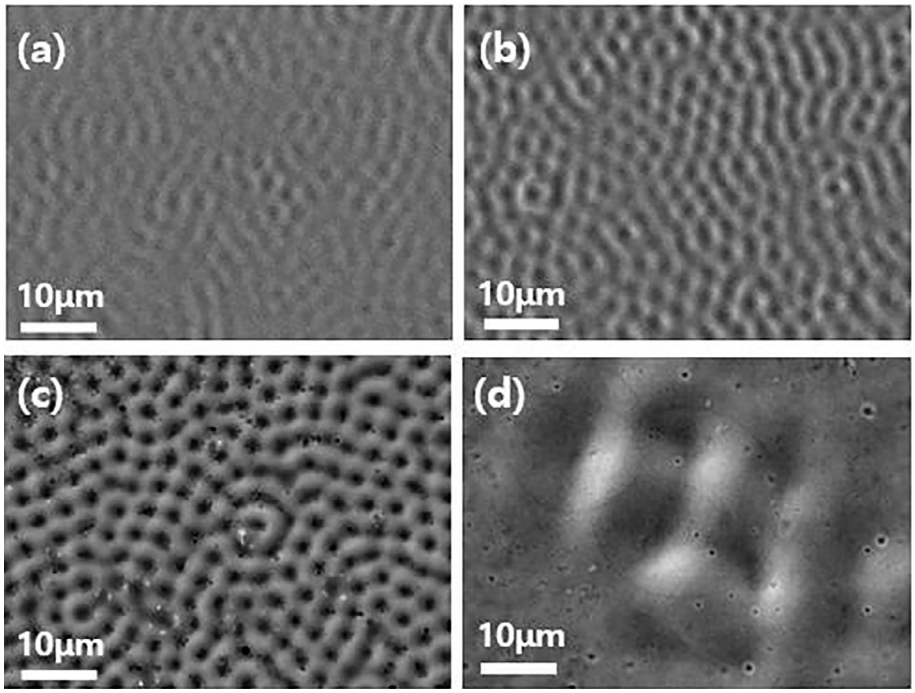

Fig. 1. SEM images of silicon wafer surface irradiated by laser pulses under DI water, (a) 30 s (600 pulses), (b) 50 s (1,000 pulses), (c) 2 min (2,400 pulses), and (d) 3 min (3,600 pulses) exposure.

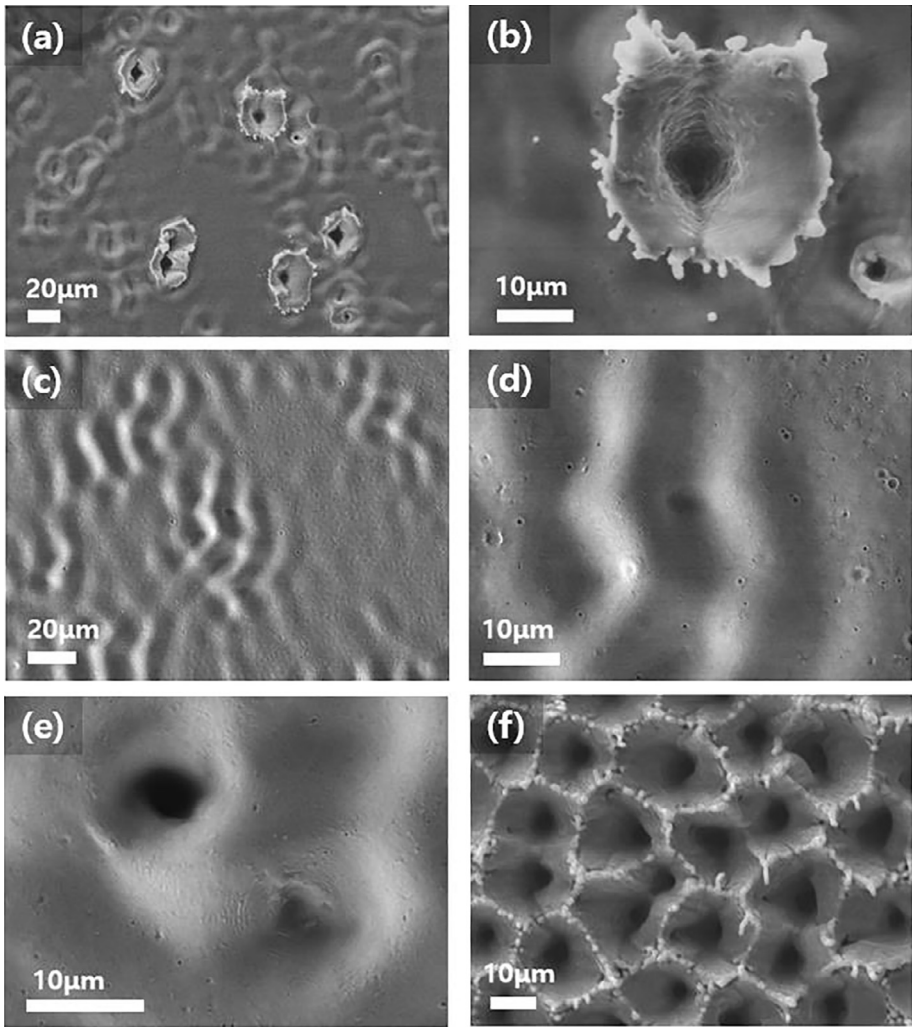

Fig. 2. SEM images of the process of forming macro expansion by time evolution. (a) 4 min (4,800 pulses). The explosions on the surface have occurred. The ripple structure of early stage and macro-scaled exploded cell exists together. (b) Magnified image of (a). The eruptive craters and ejected particles after the surface explosions. (c) 7 min (8,400 pulses). Modulated concaves are going down with melting remains at the bottom and finally hole is formed after subsidence. (d) Magnified image of (c). (e) A more developed concave feature and the stage before the concave feature formation. (f) After 20 min (24,000 pulses). Particle on the rod at the top of the wall after forming the irregular concave cells.

honeycomb of natural hexagonal structure that is changed from round cells through the thermal adjustment in the wall of unit cell [19].

After 20 min of exposure, particles and hair-like rod are found on the wall of unit cell as shown in Fig. 2f. For the feature of protruding structure, vaporization and droplet-away with particlization [16] actively occur on the wall of the concave cell. On the other hand, concave area gradually turns into a deeper and larger circular cone-shaped holes because of melting and etching with localized high density energy [18]. As the eroding of unit cell by vaporization brings a steeper slope of the wall, breakdown of the walls starts at the center of the beam spot after 15 min of exposure.

Fig. 3 contains the various stages of silicon surface modification by 1 h of irradiation. Energy dependence of surface morphology evolution is exhibited with a magnified image (Fig. 3a) from the center of the beam (right side) to the outer boundary. At the outer boundary with low fluence, capillary ripples are shown like frozen waves on the surface (Fig. 3b). More evident changes of grooves are observed with holed-concave surface structure in the inner side of the beam (Fig. 3c). Polyhedral cell arrangement with vivid edge of a unit cell is located in the center area of the beam (Fig. 3e). The breakdown of the separation walls results in the complicated eroding structure at the center of the beam (Fig. 3f).

Air does not transfer much thermal energy owing to low density and low conductivity [20]. When the laser beam with low fluence shines onto silicon wafer in a water medium, water on the surface of silicon behaves like a laminar heat reservoir [21] which can keep the much large amount of radiant heat from the silicon because of high density (1,000 times higher than air), high specific heat (6 times than Si, 4 times than air) and high conductivity (over 20 times than air). Accordingly, water has a steep thermal gradient against ambient medium and its temperature does not change rapidly due to the low thermal conductivity (200 times lower than Si) so that 'heat cover' [21] layer with small heat affected zone exists at the interface between silicon and water. This region leads to thermodynamic strain and causes surface roughness modulation on the silicon surface [16].

While the silicon surface is being cooled by water, the temperature inside silicon rises above the surface temperature and superheated liquid state [22,23] is proceeded by subsurface heating due to the limited absorption depth of the laser beam. Thus the heat exchange occurs to compensate this thermal difference, which is manifested by modulation of the surface with local expansions (see Fig. 4a). Repeated short-term thermal gradients by laser pulses give gradual changes in the initial orientation of the molecules by shear stress. As a result, because of the difference of the thermal conductivity, the heat flux is deflected from the normal direction to form ripple patterns.

Whereas the local expansion is caused by the distribution of the thermal wave at the interface between the silicon surface and water, the creation of the macro expansion is slightly different. When a laser beam incident onto a material, photons transfer the thermal energy into the lattice of material. Due to the water, remaining thermal energy not dissipated through the surface contributes to the volume heating which causes the expansion and change of the lattice structure.

Although the laser-induced heat in silicon dissipates and temperature distribution is uniform, consecutive laser pulses may gradually

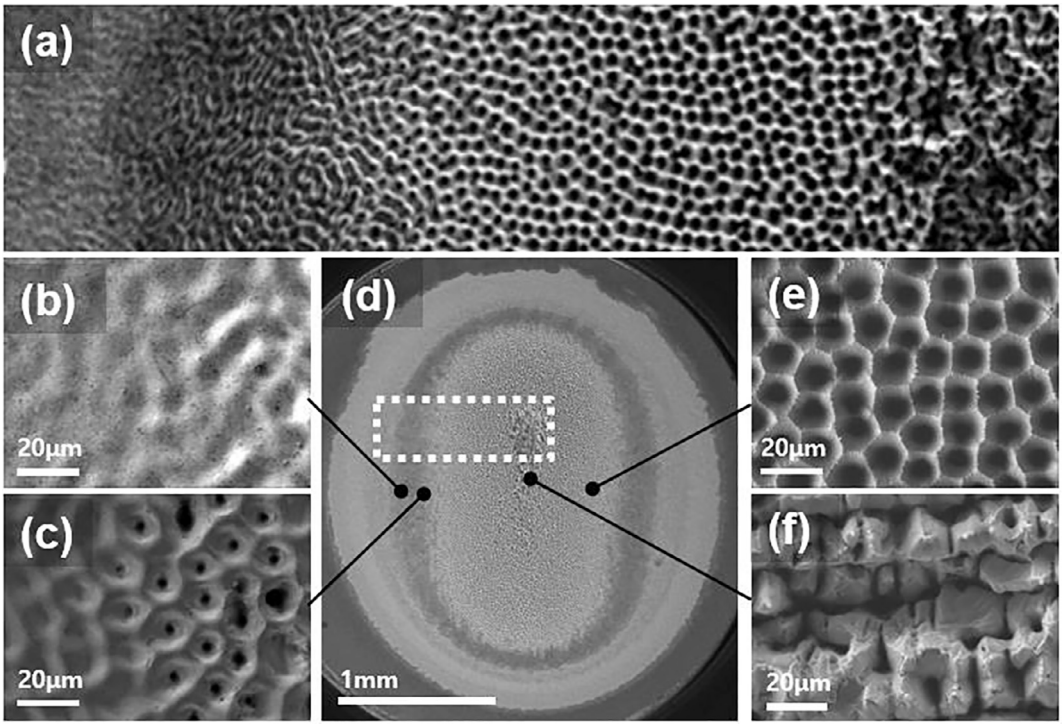

Fig. 3. SEM images of a representative area of 1 h (72,000 pulses) exposed silicon surface in a water medium, (a) Magnified image of the dashed rectangular area in (d), (b) Capillary wave formation in outer areas, (c) Concaves and holes in the boundary area, (d) Full image of the beam spot on the silicon surface, (e) Porous structure in the inner area, (f) Breakdown of the wall of the unit cell in the center.

change the optical and thermophysical properties of silicon. Thus, the following pulse comes to a modified surface that can be important for the formation of the observed structures under the multi-pulse irradiation conditions. During the expansion, subsurface heating widens the gap among the molecules to form space and promote void growth.

Inside the surface with high thermal energy, mass transportation is more effective than diffusion in order to solve the thermal imbalance with the outside, which forms the thermal strain of the molecules and forms the molten area due to defects of the lattices [16]. Naturally, a complex type of heat exchange system finally forms a heat exchange cell having a hexagonal pattern like Rayleigh-Benard convection. The difference of the thermal flux changes the optical absorption coefficient of the material, which accelerates the modulation of the material. The coalescence of the voids leads to a volume expansion and forms break

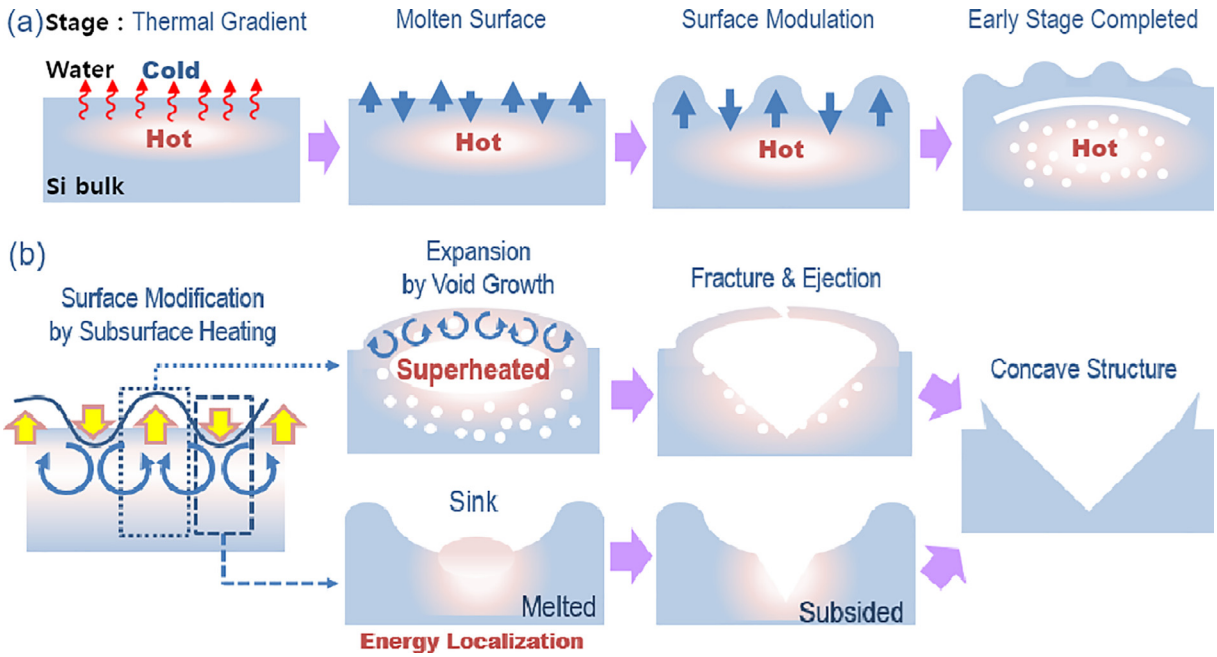

Fig. 4. A schematic diagram of the process (a) Local expansions at the early stage. Wavy and filled arrow symbols represent the direction of the thermal gradient and surface deformation at local expansion. (b) A macro expansion by subsurface heating. Blank and round arrow symbols represent the direction of the surface deformation in macro expansion and thermodynamic strain.

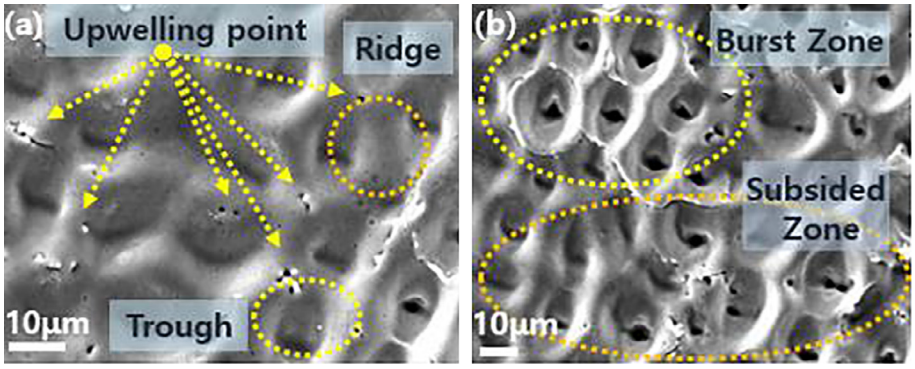

Fig. 5. Images of modulated silicon surface of (a) ridge and trough structure, (b) explosion zone and subsided zone.

points at the relatively cold surface. At this time, the substances in the superheated liquid state of the subsurface undergo rapid phase transition, and ejection occurred. As a result, it remains the concave porous structure with the distorted hexagonal arrangement. Whereas, on the unexpanded concave surface, the subsurface heated area is easily perforated owing to the energy concentration [18] by the curved surface and enters deeply in the depth direction (see Fig. 4(b)).

After receiving the large amount of energy from the heated surface due to the high specific heat, water has a steep thermal gradient with low thermal conductivity. In order to resolve the thermal difference at the cold water side far from the surface, mass transportation by density results in convective flows. This thermal instability affects the thermal distribution over the surface by organizing the distorted thermodynamic hexagonal cell formation with the unit cell having cold and hot area. Thermodynamic formation is attributed to surface tension gradients to cause the shear stress in the phase boundary of silicon so that irregular cell formation appears on the silicon surface.

Fig. 5 shows the typical features of the expansion by thermodynamic convection. On the top of the ridge, there is a heat stagnation point [11], where the heat stagnates and the temperature drops. Accordingly, this area has high tensile force to make the breakup point, and then remains the upwelling point with cavity. Ridges were formed by surface expansion in hot areas while troughs in cold areas (Fig. 5a). They make the groove following their thermal distribution and finally make the typical form of g-type Rayleigh-Benard convection [25] that rises on the edges and sinks in the center. Thus, the results can support the idea that convective flow existed inside of material during superheated state.

Status of thermal circulation in a unit cell can be confirmed by calculation of Prandtl number defined by kinematic viscosity ν over thermal diffusivity α. ($\nu = \mu/\rho$, $\alpha = \kappa/(\rho C_{p,})$, κ is thermal conductivity, $C_{p,}$is specific heat, Prandtl number = $\nu/\alpha = \mu/(\rho\alpha)$). According to silicon viscosity μ of around 0.75 [mPa·s] at melting temperature [24], silicon density ρ and diffusivity α of 0.8 [cm^2/sec], Prandtl number of molten silicon becomes 0.00365. This value is much smaller than the critical Prandtl number so it belongs to g-type hexagonal formation [25] that has the inflated boundary of each cell. This explains the shape of the macro expansion when it begins to occur. Thus, we can distinguish the macro expansion of the embossed form by partial heating at an early stage from the macro expansion applied by the convection mechanism.

The explosions on the surface occur mainly in the trough area, although homogeneous nucleation by subsurface heating [22,23] is taken place equally by absorbing the same amount of energy through the same area. It is not only the reason that cold area has higher surface tension than hot area, but energy is also localized at the trough of the surface [18]. Therefore, the explosion zone naturally accompanied with the sinking zone (Fig. 5b) can be seen in the porous structure.

The silicon surface was examined with an AFM to clarify the formation of the macro expansion. Fig. 6a and 6b shows the top view and

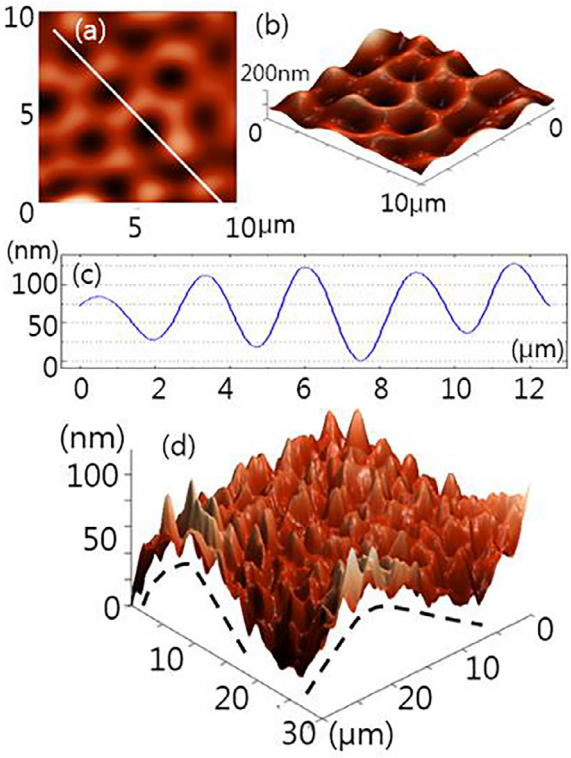

Fig. 6. AFM images of silicon wafer surface after laser irradiation of 50 s (1,000 pulses). (a) Top view of the surface shows honeycomb-like array pattern, (b) Perspective view helps to see a more realistic feature on the surface, (c) Surface roughness along the line in (a). It shows the period of 2–3 μm and height of 50–150 nm, (d) Perspective view with modified height scale of nanometer. Dotted lines show that macro expansions occur concurrently under local expanded cells of 2–3 μm.

the perspective view of the regular porous structure after laser irradiation of 50 s, respectively. Fig. 6c shows the surface roughness along the line in 6a and period of 2–3 μm. As can be seen in Fig. 6d, the macro expansions (black dotted line) are proceeding with the local expansions at the early stage of the surface modulation progress. It is obviously disclosed that surface modulation starts with spike-like (actually inflated wall of the unit cell) local growth to remove the thermal energy and makes round cell formation by thermal convective temperature distribution macroscopically. Interestingly, the local expansion on the macro expansion can be morphologically recognized as surface tension-dominant Marangoni convection [10,11] that is bound to the surface. The macro subsurface expansion by the penetrating volume heating is of about 10–20 μm and the local expansion is of about 2-μm period on the surface. Therefore, it was found that the hierarchical structure built

up by laser exposure was proceeding with two different scales simultaneously.

Conclusion

We demonstrated that pulsed nanosecond laser interaction with silicon in aqueous medium can produce self-organized microporous array structure and investigated the time-dependent morphology evolution. Any chemicals and auxiliary equipment are not necessary to produce this structure except laser and water.

The thermal gradient formed by the laser in a short time causes the shear strain and induces the deformation of the lattice structure on the molecular scale. These initially created lattice defects and provided a critical starting point for subsequent shape deformation. The accumulation of gradual changes of solid surface in these microscopic time scales completes the general thermodynamic law seen on the liquid surface in macroscopic time scale.

We have made the concave cone-shaped porous structure by using the surface explosions like a boiling surface and this is supposed to be the helpful attempt for elucidating the phenomena for further researches.

Acknowledgements

This work was supported by the National Research Foundation of Korea (NRF) grants funded by the Korean Government (MSIP) [grant numbers NRF-2015M2A2A4A03044653, 2015R1A5A1009962, and 2016K1A3A1A61005950].

References

[1] Parretta A, Sarno A, Tortora P, Yakubu H, Maddalena P, Zhao J, et al. Angle-dependent reflectance measurements on photovoltaic materials and solar cells. Opt Commun 1999;172:139–51. https://doi.org/10.1016/S0030-4018(99)00561-1.

[2] Qiu XJ, Tan XW, Wang Z, Liu GY, Xiong ZH. Tunable, narrow, and enhanced electroluminescent emission from porous-silicon-reflector-based organic microcavities. J Appl Phys 2006;100:074503https://doi.org/10.1063/1.2355536.

[3] Collart-Dutilleul P, Secret E, Panayotov I, Deville de Périère D, Martín-Palma R, Torres-Costa V, Martin M, Gergely C, Durand J, Cunin F, Cuisinier F. Adhesion and proliferation of human mesenchymal stem cells from dental pulp on porous silicon scaffolds. Appl Mater Interf 2014;6:1719–28. https://doi.org/10.1021/am4046316.

[4] Harraz F. Porous silicon chemical sensors and biosensors: a review. Sensor Actuat B-Chem 2014;202:897–912. https://doi.org/10.1016/j.snb.2014.06.048.

[5] Li L, Zhao X, Wong C-P. Deep etching of single- and polycrystalline silicon with high speed, high aspect ratio, high uniformity, and 3D complexity by Electric Bias-Attenuated Metal-Assisted Chemical Etching (EMaCE). ACS Appl Mater Interf 2014;6(19):16782–91. https://doi.org/10.1021/am504046b.

[6] Ensafi A, Ahmadi N, Rezaei B, Abarghoui M. A new electrochemical sensor for the simultaneous determination of acetaminophen and codeine based on porous silicon/palladium nanostructure. Talanta 2015;134:745–53. https://doi.org/10.1016/j.talanta.2014.12.028.

[7] Asoh H, Arai F, Ono S. Effect of noble metal catalyst species on the morphology of macroporous silicon formed by metal-assisted chemical etching. Electrochim Acta 2009;54:5142–8. https://doi.org/10.1016/j.electacta.2009.01.050.

[8] Trtica MS, Gakovic BM, Radak BB, Batani D, Desai T, Bussoli M. Periodic surface structures on crystalline silicon created by 532nm picosecond Nd:YAG laser pulses. Appl Surf Sci 2007;254:1377–81. https://doi.org/10.1016/j.apsusc.2007.06.050.

[9] Vorobyev AY, Makin VS, Guo C. Periodic ordering of random surface nanostructures induced by femtosecond laser pulses on metals. J Appl Phys 2007;101:034903https://doi.org/10.1063/1.2432288.

[10] Getling AV. Rayleigh - Bénard Convection: Structures and Dynamics. Singapore: World Scientific; 1998.

[11] Duh JC, Yang WJ. Numerical analysis of natural convection in liquid droplets by phase change. Numer Heat Transfer 1989;15:129–54. https://doi.org/10.1080/10407788908944710.

[12] Lu Q, Mao SS, Mao X, Russo RE. Delayed phase explosion during high-power nanosecond laser ablation of silicon. Appl Phys Lett 2002;80:3072. https://doi.org/10.1063/1.1473862.

[13] Garrison Barbara J, Itina Tatiana E, Zhigilei Leonid V. Limit of overheating and the threshold behavior in laser ablation. Phys Rev E 2003;68:041501https://doi.org/10.1103/PhysRevE.68.041501.

[14] Yang L, Dolnik M, Zhabotinsky AM, Epstein IR. Turing pattern beyond hexagons and stripes. Chaos 2006;16:037114https://doi.org/10.1063/1.2214167.

[15] Cross MC, Hohenberg PC. Pattern formation outside of equilibrium. Rev Mod Phys 1993;65:851. https://doi.org/10.1103/RevModPhys. 65.851.

[16] Brailovsky AB, Gaponov SV, Luchin VI. Mechanisms of melt droplets and solid-particle ejection from a target surface by pulsed laser action. Appl Phys A 1995;61:81–6. https://doi.org/10.1007/BF01538216.

[17] Bauerle D. Laser Processing and Chemistry. 3rd ed. Berlin: Springer; 2000. p. 691.

[18] Pedraza AJ, Jesse S, Guan YF, Fowlkes JD. Laser-induced surface perturbations in silicon. J. Mater. Res. 2001;16(12):3599–608. https://doi.org/10.1557/JMR.2001.0493.

[19] Karihaloo BL, Zhang K, Wang J. Honeybee combs: how the circular cells transform into rounded hexagons. J R Soc Interf 2013. https://doi.org/10.1098/rsif.2013.0299.

[20] William M. Haynes, CRC handbook of chemistry and physics. 95th ed. CRC Press; 2014.

[21] Mak Giuseppe Y, Lam Edmund Y, Choi HW. Liquid-immersion laser micromachining of GaN grown on sapphire. Appl Phys A 2011;102:441–7. https://doi.org/10.1007/s00339-010-6169-z.

[22] Bulgakova NM, Bulgakov AV. Pulsed laser ablation of solids: transition from normal vaporization to phase explosion. Appl Phys A 2001;73:199–208. https://doi.org/10.1007/s003390000686.

[23] Singh RK, Bhattacharya D, Narayan J. Subsurface heating effects during pulsed laser evaporation of materials. Appl Phys Lett 1990;57:2022. https://doi.org/10.1063/1.104118.

[24] Sasaki H, Tokizaki E, Huang XM, Terashima K, Kimura S. Temperature dependence of the viscosity of molten silicon measured by the oscillating cup method. Jpn J Appl Phys 1995;34:3432. https://doi.org/10.1143/JJAP.34.3432.

[25] Thess A, Bestehorn M. Planform selection in Benard-Marangoni convection - l hexagons vs g hexagons. Phys Rev E 1995;52:6358. https://doi.org/10.1103/PhysRevE.52.6358.